

## Postulated Tsunami Propagation and Inundation Analyses of Nuclear Power Plant Sites in South Korea using COMCOT code

Taesoo Choi <sup>a\*</sup>, Pil Kwon <sup>b</sup> and Eung Soo Kim <sup>a\*</sup>

<sup>a</sup>Dept of Nuclear Engineering, Seoul National University, 559 Gwanak-ro, Gwanak-gu, Seoul

<sup>b</sup>Naver Maps corps, Green factory, 6, Buljeong-ro, Bundang-gu, Seongnam-si, Gyeonggi-do

\*Corresponding author: kes7741@snu.ac.kr

### 1. Introduction

Since a large tsunami struck and damaged Fukushima Nuclear Power Plant (NPP) site in 2011, the research demand on the potential effects and mitigation measures of tsunami at NPP sites has been increased. In South Korea, there are 3 NPP sites on the east coast where large tsunami could strike.

This study analyzes tsunami behavior near Nuclear Power sites on the south-east coast of Korea (Kori, Wolsung and Ulchin). The behavior of tsunami depends on the faults location, geological characteristics and under marine topography in propagation path. In this study, Faults zones in west Japan were selected as tsunami sources. Faults surface geometry was derived with empirical correlation model and investigated data. Topography data with different resolution was collected to save computational cost. From tsunami initiation to inundation simulation, tsunami simulation code Cornell Multi-grid Coupled Tsunami model v1.7 (COMCOT) was used. Analysis cases consists of historical earthquakes and potential earthquakes.

Analysis was conducted on the tsunami height for long time period for which tsunami can reach at Analysis area. The propagation velocity and the propagation pattern according to time series near NPP sites were simulated. Through the results of this study, it is expected that a database on tsunami height could be constructed, and it will contribute to the construction of a prediction system for the arrival time and height of tsunami.

### 2. Fault modeling and Generating Input data

Tsunamis generated in west Japan has influenced the east coast of Korea. Fault zone region where earthquakes occurred frequently were designated and analysis faults were selected in each region. To consider tsunami physics depending on water depth, Various resolution topography data were adopted.

#### 2.1 Fault zones designation and Geological Modeling

The fault information in the East sea was collected from the United States Geological Survey (USGS) database. Fault information has been collected for earthquakes with a magnitude of 6.0 or more in the East Sea since the 1960s. Two fault zone were designated in west Japan. Based on Fig. 1, the occurrence of earthquakes in the East Sea was observed to be concentrated in the west side of Japan, designated as Region 1 and Region 2.



Fig. 1. Fault zone designation  
Earthquakes above Mw. 6.0 after 1960s were plotted

Fault parameter which cannot be obtained from the USGS was estimated with the model that correlate the momentum magnitude and fault dislocation [1].

$$M_0 = \mu \bar{D} A \quad (1)$$

$$M_w = \frac{2}{3} \log_{10}(M_0) - 10.7 \quad (2)$$

where  $M_0$  is the seismic moment,  $A$  is the rupture surface, and  $\bar{D}$  is the dislocation. The shear modulus ( $\mu$ ) can be determined by the material property of the fault plane. The surface rupture length(SRL) and rupture area were derived from equation (3) and (4) [2].

$$\log(SRL) = -3.22 + 0.69M_w \quad (3)$$

$$\log(RA) = -3.49 + 0.91M_w \quad (4)$$

#### 2.2 Acquisition of topography and grid construction

The Tsunami wave is highly affected by submarine topography. To consider non-linear effect of tsunami and computational efficiency, multi-grid topography was used in this study. The entire area was divided into three-level layers. Layer-1 covers tsunami propagation at oceanic scale. Layer-2 represented the east coastal line of South Korea and Ulleung basin. These area has large gradient of bathymetry which affect wave diffraction and wave breaking. Layer-3 contained the area near the NPP sites divided into Layer-3A, 3B and 3C. Each layer

represents Kori, Wolsung and Ulchin NPP sites. Spatial resolution of layers are 1-minute, 1/8-minute and 1/64-minute (about 30m). The XYZ topography data of the analysis area based on latitude-longitude system was obtained from National Oceanic and Atmospheric Administration (NOAA) and National Geographic Information Institute of Korea (NGII) database. post-processing was done with GIS program ArcGIS.

### 3. Numerical code and analysis condition

#### 3.1 Selection of Simulation code

COMCOT v1.7 was used for analyzing the entire lifespan of tsunami from initiation to run-up. This code is suitable to simulate global-scale tsunami simulation because the spherical coordinate system and longitude-latitude system were adopted. Initial tsunami height and direction are calculated with Okada model [3], and a Coriolis force is considered during wave propagation.

#### 3.2 Governing equation

The Shallow Water Equation(SWE) and bottom friction equation are the main governing equations [4]. SWE consists of a continuity equation and momentum equation as shown in equation (5) to (7). Friction force can be calculated with equation (8) and (9) Where  $\eta$  is water elevation, P and Q is volume flux toward x and y direction.  $F_x, F_y$  represents friction force, and  $\varphi, \psi$  are latitude and longitude. Coriolis force is represented as  $f$  in momentum equation. The form of momentum equation can be determined depending on considering non-linear convective term. The non-linearity should be considered at coastal region and depth rapidly changing area.

$$\frac{\partial \eta}{\partial t} + \frac{1}{R \cos \varphi} \left\{ \frac{\partial P}{\partial \psi} + \frac{\partial}{\partial \varphi} (\cos \varphi Q) \right\} = -\frac{\partial h}{\partial t} \quad (5)$$

$$\frac{\partial P}{\partial t} + \frac{1}{R \cos \varphi} \frac{\partial}{\partial \psi} \left\{ \frac{P^2}{H} \right\} + \frac{1}{R} \frac{\partial}{\partial \varphi} \left\{ \frac{PQ}{H} \right\} + \frac{gH}{R \cos \varphi} \frac{\partial \eta}{\partial \psi} - fQ + F_x = 0 \quad (6)$$

$$\frac{\partial Q}{\partial t} + \frac{1}{R \cos \varphi} \frac{\partial}{\partial \psi} \left\{ \frac{PQ}{H} \right\} + \frac{1}{R} \frac{\partial}{\partial \varphi} \left\{ \frac{Q^2}{H} \right\} + \frac{gH}{R} \frac{\partial \eta}{\partial \varphi} + fP + F_y = 0 \quad (7)$$

$$F_x = \frac{gn^2}{H^{7/3}} P(P^2 + Q^2)^{1/2} \quad (8)$$

$$F_y = \frac{gn^2}{H^{7/3}} Q(P^2 + Q^2)^{1/2} \quad (9)$$

Wave propagation was analyzed with linear SWE at Layer-1 and non-linear SWE at Layer-2 and Layer-3

#### 3.3 Selection of faults for analysis

Three historical earthquakes were selected in each region. Earthquakes in region 2 has larger magnitude than those in region 1. The information of largest earthquakes in each region is represented in Table I.

Table I. Historical fault geometry information

	F1-1	F2-1
Magnitude	6.8	7.7
Depth [km]	370.5	25.5
Length [km]	29.65	123.880
Width [km]	16.827	26.546
Dislocation[m]	1.188	4.035
Strike angle [°]	290	356
Dip angle[°]	48	48
Rake angle[°]	-11	88
location[°]	[36.808, 134.850]	[42.851, 139.197]
Date	2007.07.16	1993.07.12

For conservative analysis condition, this study modified some information such as magnitude and strike angle based on the historical faults. In case of postulated faults in Region 1, epicenter near north Sadoga island was designated where sedimentary layers show the evidence of large faults. Magnitude was increased to 7.5 and 7.8. For faults in Region 2, fault strike angle was modified to face Korea peninsula while the other parameters were maintained. In addition, it is assumed that several earthquakes in certain region take place at the same time. Location of faults and Layers is as shown in Fig. 2.

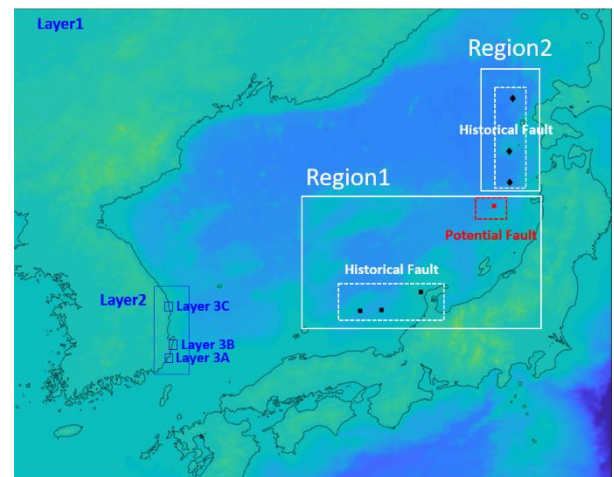


Fig.2 Analysis layer configurations  
Location of faults and layers is plotted.

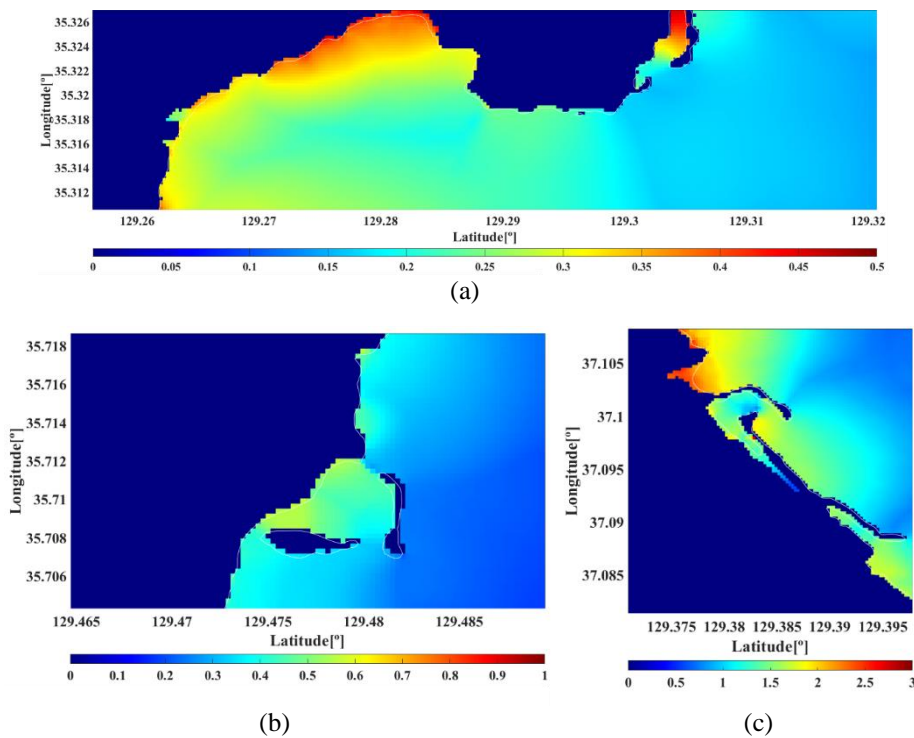


Fig.3 Maximum height near NPP sites for Region 1 postulated earthquake.  
(a) Layer 3-A Kori NPP (b) Layer 3-B Wolsung NPP (c) Layer 3-C Ulchin NPP

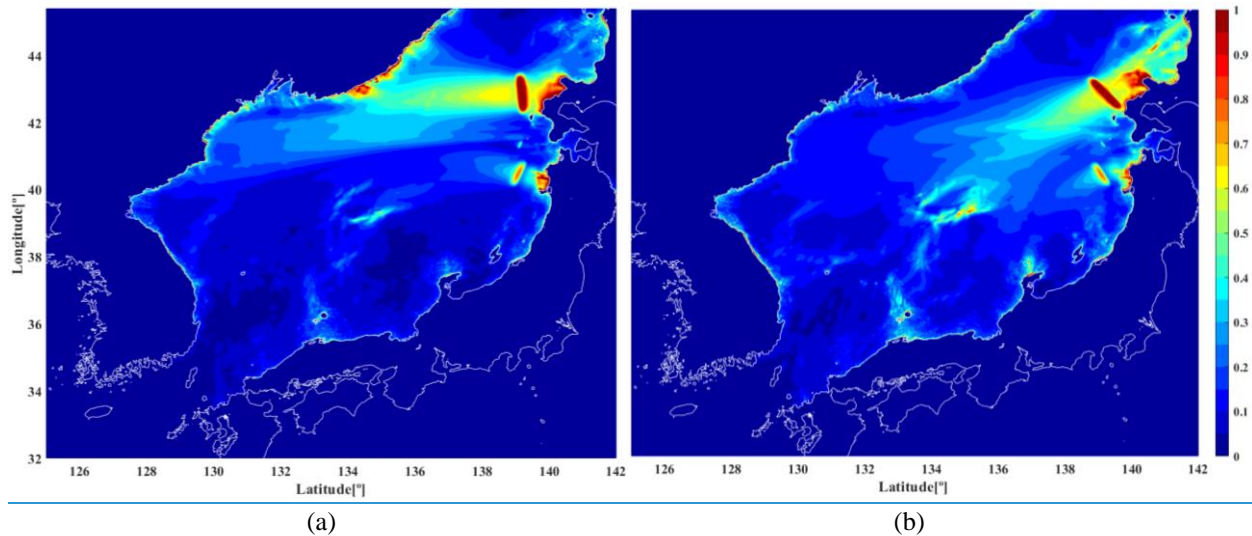


Fig.4 Maximum height at Layer-1 scale for Region 2 (a) historical earthquakes and (b) postulated earthquake

#### 4. Results of Simulation

In this study, the maximum/minimum height and flooding in the vicinity of the NPP sites were evaluated. Tsunami from historical earthquakes in region1 reaches the South Korea peninsula approximately 6000s after earthquakes happen. The maximum height of tsunami is estimated to be less than 0.01m for all NPP shore. The region of tsunami occurrence has shallow water depth, so initial water surface dislocation could not produce enough volume flux. In addition, the energy of tsunami was dissipated during propagation into the shallow water

region of west Japan. The analysis case of Mw 7.8 postulated earthquake at north Sadoga island in Region 1 shows that tsunami developed up to 2.7m near Ulchin NPPs site as shown in Fig. 3.

In case of Tsunami from Region 2, Maximum height was measured near Ulchin NPP site. For historical case, maximum and minimum height were measured as 1.5913m/-2.0421m. When strike angle was modified,

Tsunami near Ulchin NPP site develop up to 2.1590m/-2.5272m. Otherwise, Tsunami height near Kori and Wolsung NPPs didn't exceed 1m in both cases. The wave was dissipated during much longer distance than region

1 and diffracted due to submarine topography of East sea. This analysis results about propagation pattern and diffraction are similar to previous study dealing with earthquakes near Region 1 and 2 [5] which showed the wave was mainly diffracted toward northern coast of Korea and western Japan. For all analysis cases, Inundation did not occur in NPP sites.

### **5. Conclusion**

This study investigates the propagation of potential tsunamis occurring in northwest and Midwest Japan. For earthquakes magnitude 6.0 or above, maximum and minimum wave height near Kori, Wolsung and Ulchin NPP sites were calculated. The maximum height of wave was measured near Ulchin NPP sites. However, the wave height didn't exceed height of NPP sites, inundation was not found for all analysis cases. Because the analysis result doesn't consider wave breaking phenomena in coastal region, this prediction can be interpreted as conservative. From these reasons, it can be concluded that the risk of inundation and flooding is very low at the NPP site in south and east coast of Korea

### **REFERENCES**

- [1] Kanamori, Hiroo. "The energy release in great earthquakes." *Journal of geophysical research* 82.20 (1977): 2981-2987..
- [2] Wells, Donald L., and Kevin J. Coppersmith. "New empirical relationships among magnitude, rupture length, rupture width, rupture area, and surface displacement." *Bulletin of the seismological Society of America* 84.4 (1994): 974-1002..
- [3] Okada, Yoshimitsu. "Surface deformation due to shear and tensile faults in a half-space." *Bulletin of the seismological society of America* 75.4 (1985): 1135-1154.
- [4] Wang, Xiaoming. "User manual for COMCOT version 1.7 (first draft)." *Cornel University* 65 (2009).
- [5] Satake, Kenji. "Effects of bathymetry on tsunami propagation: Application of ray tracing to tsunamis." *Pure and Applied Geophysics* 126.1 (1988): 27-36